Published for SISSA by Springer

Received: *July 28, 2023*
Revised: *October 26, 2023*
Accepted: *November 13, 2023*
Published: *November 23, 2023*

Axionic domain walls at Pulsar Timing Arrays: QCD bias and particle friction

Simone Blasi,[a] Alberto Mariotti,[a] Aäron Rase[a] and Alexander Sevrin[b,c]

[a] *Theoretische Natuurkunde and IIHE/ELEM, Vrije Universiteit Brussel, & The International Solvay Institutes, Pleinlaan 2, B-1050 Brussels, Belgium*

[b] *Theoretische Natuurkunde, Vrije Universiteit Brussel, & The International Solvay Institutes, Pleinlaan 2, B-1050 Brussels, Belgium*

[c] *Universiteit Antwerpen, Prinsstraat 13, 2000 Antwerpen, Belgium*

E-mail: simone.blasi@vub.be, alberto.mariotti@vub.be, aaron.rase@vub.be, alexandre.sevrin@vub.be

Abstract: The recent results from the Pulsar Timing Array (PTA) collaborations show the first evidence for the detection of a stochastic background of gravitational waves at the nHz frequencies. This discovery has profound implications for the physics of both the late and the early Universe. In fact, together with the interpretation in terms of supermassive black hole binaries, many sources in the early Universe can provide viable explanations as well. In this paper, we study the gravitational wave background sourced by a network of axion-like-particle (ALP) domain walls at temperatures around the QCD crossover, where the QCD-induced potential provides the necessary bias to annihilate the network. Remarkably, this implies a peak amplitude at frequencies around the sensitivity range of PTAs. We extend previous analysis by taking into account the unavoidable friction on the network stemming from the topological coupling of the ALP to QCD in terms of gluon and pion reflection off the domain walls at high and low temperatures, respectively. We identify the regions of parameter space where the network annihilates in the scaling regime ensuring compatibility with the PTA results, as well as those where friction can be important and a more detailed study around the QCD crossover is required.

Keywords: Axions and ALPs, Early Universe Particle Physics, Phase Transitions in the Early Universe

ArXiv ePrint: 2306.17830

https://doi.org/10.1007/JHEP11(2023)169

JHEP11(2023)169

Contents

1 Introduction

The PTA consortium has very recently reported the first positive evidence of a stochastic gravitational wave background (SGWB) around the nHz frequency [1–9] (see [10–14] for previous PTA results). One possibility is that this signal is of astrophysical origin and that it consists of a superposition from super massive black hole binaries [15]. However, it is interesting to explore the possibility that the background observed at PTAs is actually of cosmological origin. In this case, this discovery would provide unique new information about the early history of our Universe. Several works have recently appeared, with the aim of interpreting this new SGWB signal at PTAs [16–33], for previous studies see e.g. [34–50]. The NANOGrav collaboration has already considered several new physics interpretations of their dataset as well [1].

In this paper, we focus on the scenario where the detected SGWB is sourced by domain walls (DWs), namely two-dimensional topological defects that can arise during a phase transition involving the spontaneous breakdown of a discrete symmetry [51, 52]. DW networks are predicted in many scenarios of physics Beyond the Standard Model (BSM) and their signatures have been recently investigated in several works [37, 43, 46, 47, 50, 53–72] (see [73, 74] for reviews on domain walls).

A DW network in the early Universe can be a powerful source of gravitational waves, as shown quantitatively in numerical simulations of the corresponding field theory [74–77]. The NANOGrav collaboration has in fact interpreted this signal as coming from a DW network in the scaling regime, identifying the ranges of temperature and energy density of the network compatible with the data [1]. We will employ their results in our analysis.

A scenario where DWs arise naturally is in models of axion-like-particles (ALPs). ALPs are generalizations of the Peccei Quinn QCD axion solving the strong CP problem [78–81], and they are common in BSM physics, see e.g. [82–99].

DWs arise naturally in ALP models where the discrete subgroup of the U(1) which is preserved by the anomaly undergoes spontaneous symmetry breaking. These DWs can be topologically stable and eventually dominate the energy density of the Universe [52, 100], in conflict with standard cosmology. This problem can be avoided by introducing a (small) explicit breaking of the discrete symmetry (the so-called *bias*), leading to the annihilation of the network [100–102]. The size of the bias is generally a new independent parameter, which determines the phenomenology of the network and in particular the emitted SGWB.

As we shall discuss, a natural scenario to motivate the signal from ALP DWs at the PTA frequencies is the one where the ALP couples to QCD, as already suggested e.g. in [47, 50, 71, 76, 103], so that the QCD-induced potential itself acts as a bias. In this case, however, friction from the QCD sector in the thermal plasma is inevitable. Determining the impact of this friction force for the ALP domain wall interpretation of the PTA data is the main goal of our study (see [71, 73, 104–106] for previous studies of friction effects on DW networks). In fact, when friction dominates the network departs from scaling and the corresponding SGWB can significantly change with respect to the one observed in numerical simulations [74–77] where plasma effects are not included.

Our main result is that friction acting on the DWs from the QCD sector can in general be relevant for a significant part of the parameter space capable of explaining the NANOGrav signal, and that a departure from the scaling regime (on which the PTA interpretation is based) is possible, even though a more detailed analysis around the QCD crossover is required to completely settle the issue. We also find parameter space compatible with the SGWB at PTAs where friction can be safely neglected.

Note that our study focusses on a minimal realization of ALP DWs with QCD-induced bias, where the heavy ALP cannot be the QCD axion. Nevertheless our analysis on friction effects can apply equally to non-minimal scenarios where the heavy axion is actually the one responsible to solve the strong CP problem, see e.g. [53, 107, 108].

Additionally, while the study presented in this paper focuses on the unavoidable coupling with QCD, friction could also impact the DW network if other ALP-SM (model-dependent) couplings are present. For instance, in ref. [71] it was shown that if the ALP couples to muons[1] the resulting friction can actually play a role at PTA frequencies provided that this interaction has the right strength.

The structure of the paper is as follows. In the next section we review the basics of ALP domain walls and SGWBs. Then, in section 3 we show that ALP DWs whose bias is induced by QCD are a natural candidate to explain the PTA signal, by comparison with the model-independent analysis in [1]. In section 4 we study the impact of friction from the QCD sector, analyzing the contribution from gluons and pions at high and low temperatures. In section 5 we present our results showing the relevance of friction for the ALP parameter space.

[1]The other SM fermions are either too weakly coupled (the light ones), or generally too heavy to be abundant in the plasma at the QCD crossover.

JHEP11(2023)169

2 ALP domain walls

We consider domain walls that generically arise in ALP models. We introduce our notation and setup. We start off by considering a dark QCD non abelian group SU(N) and a U(1) Peccei-Quinn symmetry anomalous under SU(N). The corresponding pseudo-Nambu-Goldstone boson, a, plays the role of the ALP in our analysis. The Lagrangian for the ALP contains the following term

$$\mathcal{L}_a \supset \frac{\alpha_d}{4\pi}\frac{N_d}{v} a\, G_d \widetilde{G}_d, \tag{2.1}$$

where α_d is the dark gauge coupling constant, v is the U(1) breaking vev, and G_d is the dark gauge boson field strength, which is contracted with its dual $\tilde{G}_d$. In terms of the quantities above it is useful to define the ALP decay constant f_a as

$$f_a = \frac{v}{N_{\rm DW}}, \qquad N_{\rm DW} = 2N_d. \tag{2.2}$$

In terms of this quantity the Lagrangian is defined as usual as

$$\mathcal{L}_a \supset \frac{\alpha_d}{8\pi}\frac{a}{f_a} G_d \tilde{G}_d. \tag{2.3}$$

For $N_d = 1/2$ the domain wall number, $N_{\rm DW}$, is one and the vacuum manifold for the ALP potential induced by the dark gauge theory is trivial, namely it contains only one minimum as $a = 0$ and $a = 2\pi f_a = 2\pi v$ are to be identified. For $N_{\rm DW} > 1$ however the vacuum consists of disconnected points corresponding to a discrete symmetry $\mathbb{Z}_{N_{\rm DW}}$, and stable domain wall solutions exist interpolating between neighboring minima.

The most important features of the ALP potential are captured by the following shape that encodes the discrete $\mathbb{Z}_{N_{\rm DW}}$ of the ALP Lagrangian with respect to the dark sector:

$$V_d(a) = m_a^2 f_a^2 \left(1 - \cos\left(\frac{a}{f_a}\right)\right), \tag{2.4}$$

where m_a is the ALP mass. The ALP potential is defined in the range $a \in [0, 2\pi v) = [0, 2\pi N_{\rm DW} f_a)$ and it then supports $N_{\rm DW} - 1$ degenerate and inequivalent minima. The simple cosine potential allows to obtain analytical domain wall solutions,

$$a(z) = \left[2\pi k + 4\arctan(e^{m_a z})\right] f_a, \quad k = 0, 1, \ldots N_{\rm DW} - 1, \tag{2.5}$$

with energy per unit surface (tension) given by

$$\sigma_{\rm DW} = 8 m_a f_a^2. \tag{2.6}$$

In general, the ALP potential could differ significantly from the cosine shape if additional (pseudo) Nambu-Goldstone bosons exist below the dark-QCD confinement scale, as it is the case for the QCD axion, see e.g. [109]. In any case, the profiles in (2.5) can still capture most of the relevant physics of the ALP domain wall.[2]

[2] Note however that while the cosine potential predicts vanishing ALP self-reflection off the ALP domain wall, a QCD-like potential was shown to not maintain this property [71].

JHEP11(2023)169

Cosmology evolution of DW and SGWB spectrum. We assume that the PQ breaking scale v is smaller than the reheating temperature and we focus on the case in which the domain wall number is larger than one, so that the DW network is stable [100, 110].[3] At the scale of the PQ phase transition global strings associated to U(1) are formed according to the Kibble mechanism [51], see [115–118] for recent work. Subsequently, when the ALP potential becomes cosmologically relevant, that is when $3H(T_\mathrm{f}) \sim m_a$ with H the Hubble parameter, domain walls can be considered formed. The precise relation to determine T_f should take into account the temperature dependence of the axion potential generated by the dark-QCD sector. For an ALP decay constant below the Planck scale, one can show that $T_\mathrm{f} \gtrsim \sqrt{m_a f_a}$, so we consider $\sqrt{m_a f_a}$ as an estimate of T_f that will anyway play no important role in our study.

After DW formation, the energy density of the resulting string-wall hybrid network is soon dominated by the walls [73, 76]. The DWs reach then the so-called scaling regime where the energy density of the DW network redshifts as $\rho_\mathrm{DW} \sim \sigma H$, corresponding to $\mathcal{O}(1)$ DWs per Hubble patch and mildly relativistic average velocity [119–124].

A scaling network of DWs will eventually dominate the energy density of the Universe, in contrast to standard cosmology [52, 100, 125]. This occurs when $\rho_\mathrm{DW} \sim 3H^2 M_\mathrm{Pl}^2$, where $M_\mathrm{Pl} = 2.435 \times 10^{18}$ GeV is the reduced Planck mass, or in terms of temperature

$$T_\mathrm{dom} \simeq 14\,\mathrm{MeV} \left(\frac{\sigma_\mathrm{DW}^{1/3}}{100\,\mathrm{TeV}}\right)^{3/2} \left(\frac{g_*}{10}\right)^{-1/4}, \tag{2.7}$$

where we have assumed radiation domination[4] with g_* the number of relativistic degrees of freedom, and we have used $\rho_\mathrm{DW} = 2\sigma H \mathcal{A}$ with $\mathcal{A} = 0.8$ from numerical simulations [74–77].

In order to collapse the DW network before domination, one may add a bias potential ΔV that breaks explicitly the $\mathbb{Z}_{N_\mathrm{DW}}$ symmetry. We shall then define T_* as the annihilation temperature, where $T_* > T_\mathrm{dom}$ for consistency.

Note that the collapse of the DW network may produce a significant amount of primordial black holes (PBHs), potentially leading to further constraints on the model, see e.g. [66, 126]. However, the precise estimate of the resulting PBH abundance is still uncertain and depends on the underlying assumptions regarding the geometry of the DW configurations, as well as on the dynamics of the collapse. Hence we will not consider PBH constraints in what follows.

At the time of annihilation, the DW energy density normalized to the total energy density is given by

$$\alpha_* = \frac{\rho_\mathrm{DW}}{3H^2 M_\mathrm{Pl}^2} \simeq 0.02 \left(\frac{\sigma_\mathrm{DW}^{1/3}}{100\,\mathrm{TeV}}\right)^3 \left(\frac{T_*}{100\,\mathrm{MeV}}\right)^{-2} \left(\frac{g_*}{10}\right)^{-1/2}, \tag{2.8}$$

[3] For N_DW=1 the network is unstable and decays soon after formation [110–114].

[4] One could go beyond the assumption of radiation domination, i.e. $H \sim T^2/M_\mathrm{Pl}$, by defining T_dom as the temperature when $\rho_\mathrm{DW} = \rho_\mathrm{rad}$ with ρ_rad the radiation energy density and $H \sim \sqrt{\rho_\mathrm{DW} + \rho_\mathrm{rad}}/M_\mathrm{Pl}$. This leads to a $\mathcal{O}(10\%)$ correction in the temperature which we are neglecting here.

where we assumed radiation domination.[5] This definition of α_* is inspired by analogous studies of first order phase transitions, see e.g. [127], and it directly relates to the strength of the GW emission.

The annihilation temperature may be estimated by balancing the curvature pressure with the energy difference induced by the bias, namely $\Delta V \sim \sigma_{\rm DW}/R \sim \rho_{\rm DW}$, where R is the correlation length of the network, $R \sim H^{-1}$ in the scaling regime. One finds

$$T_* \simeq 270 \text{ MeV} \left(\frac{\sigma_{\rm DW}^{1/3}}{100\,\text{TeV}}\right)^{-3/2} \left(\frac{\Delta V^{1/4}}{100\,\text{MeV}}\right)^2 \left(\frac{g_*}{10}\right)^{-1/4}, \tag{2.9}$$

where we used the more precise condition $\Delta V = \mathcal{C}_{\rm ann}\, \rho_{\rm DW}$ with $\mathcal{C}_{\rm ann} \simeq 2$ from numerical simulations [74–77]. The bias is in principle a free parameter[6] that should be added to the model, and the phenomenology of the DW network can change completely depending on its size. On the other hand, the size of the bias and the corresponding phenomenology can be actually predicted if it is generated dynamically. In the next section we will in fact explore the possibility that such bias is generated by QCD.

The DW network in the scaling regime has been proven by numerical simulations [74, 76, 77] to generate a large SGWB $\Omega_{\rm gw}(f)$ with broken power law in frequency. The signal is dominated by the last moment of emission, so it depends explicitly on T_*. The signal redshifted today has the form

$$\Omega_{\rm gw}(T_*, f) = \Omega_{\rm peak} \times \begin{cases} \left(\frac{f}{f_{\rm peak}}\right)^3 & \text{if } f \leq f_{\rm peak} \\ \left(\frac{f}{f_{\rm peak}}\right)^{-1} & \text{if } f > f_{\rm peak} \end{cases} \tag{2.10}$$

with

$$\Omega_{\rm peak} \simeq 1.64 \times 10^{-6} \left(\frac{\tilde{\epsilon}_{\rm gw}}{0.7}\right) \left(\frac{\mathcal{A}}{0.8}\right)^2 \left(\frac{g_*(T)}{10}\right) \left(\frac{g_{*s}(T)}{10}\right)^{-4/3} \left(\frac{T_{\rm dom}}{T_*}\right)^4 \tag{2.11}$$

$$f_{\rm peak} \simeq 1.15 \times 10^{-9}\,\text{Hz} \left(\frac{g_*(T)}{10}\right)^{1/2} \left(\frac{g_{*s}(T)}{10}\right)^{-1/3} \left(\frac{T_*}{10\,\text{MeV}}\right), \tag{2.12}$$

where g_{*s} is the effective number of entropy degrees of freedom and we have normalized the numerical coefficient to the values obtained in numerical simulations, with $\tilde{\epsilon}_{\rm gw} = 0.7$ [74–77]. The SGWB spectrum of DW is determined by two parameters, the tension (see eq. (2.7)) and T_*.[7] Eq. (2.11) shows that the later the DW network annihilates, the larger the GW signal is. As we can see, the best T_* for PTA frequencies is in the ballpark of the QCD scale.

[5]Similarly as in footnote 4, one could consider $H \sim \sqrt{\rho_{\rm DW} + \rho_{\rm rad}}/M_{\rm Pl}$, but since the relevant temperature ranges for our model are consistent with values of $\alpha_* < 0.5$ (i.e. $\rho_{\rm DW} < \rho_{\rm rad}$) as we show in figure 1, it is safe to assume annihilation happens in a radiation dominated regime.

[6]One may for instance expect a bias term to arise from quantum gravity effects that make the starting U(1) global symmetry only approximate [128–135].

[7]There is also a mild dependence on $N_{\rm DW}$ which is encoded in $\mathcal{O}(1)$ modifications of the numerical coefficient $\mathcal{A}$ [136].

JHEP11(2023)169

3 The QCD potential as the natural bias for DWs at PTAs

Let us now consider the effect of the QCD-induced potential on the ALP model illustrated above. This comes from the anomalous coupling between the ALP and the gluons,

$$\mathcal{L}_a \supset \frac{\alpha_s}{4\pi}\frac{N_c}{v} G\tilde{G}, \tag{3.1}$$

where N_c is the color anomaly from fermions charged under QCD. In general, N_c and N_d are two independent numbers. Whenever these numbers are coprime, the degeneracy in the vacuum manifold is lifted and domain walls become metastable.

The contribution to the ALP potential from QCD at low energy can be captured within chiral perturbation theory, see e.g. [109, 137]. One finds the following leading-order potential for the ALP-pion system:

$$V(a,\pi_0) = -\frac{f_\pi^2 m_\pi^2}{m_u + m_d}\left[m_u \cos\left(\frac{a}{2f_a'} - \frac{\pi_0}{f_\pi}\right) + m_d \cos\left(\frac{a}{2f_a'} + \frac{\pi_0}{f_\pi}\right)\right], \tag{3.2}$$

with

$$f_a' \equiv \frac{N_d}{N_c} f_a. \tag{3.3}$$

Notice that since $f_a' \neq f_a$, the periodicity of the QCD potential is generally misaligned with respect to the one of the dark-QCD potential. The interactions in (3.2) follow from an ALP-dependent rephasing of the light up and down quarks that removes the ALP from the topological term, $q \to q \exp\left(i\gamma_5 \frac{a}{2f_a} Q_a\right)$ and Q_a proportional to the identity with $\mathrm{Tr}\, \mathrm{Q_a} = 1$. Notice that this choice generates no derivative interaction between the ALP and the pions at the leading order, at the price of keeping a linear mixing between the ALP and the π_0 from the potential (3.2).

Assuming that the QCD contribution is very small compared to the dark QCD one ($m_\pi f_\pi \ll m_a f_a$), the size of the bias is generically given by $|\Delta V_k| \sim m_\pi^2 f_\pi^2$. However, the bias can become parameterically small when the two sectors are almost aligned,

$$|\Delta V_k| \sim \epsilon^2 m_\pi^2 f_\pi^2\,, \tag{3.4}$$

where ϵ quantifies the alignment. For instance, a case of extreme alignment with $\epsilon \ll 1$ can be realized by taking $N_c/N_d = 1+\epsilon$. In general, there is no one-to-one correspondence between the ratio N_c/N_d and the resulting bias, and we therefore keep ϵ as a free parameter in our analysis. We however notice that scenarios with $\epsilon \ll 1$, where the life time of the network gets parameterically enhanced, require somewhat large or fine-tuned values of N_c and N_d.

Let us now turn to discuss how temperature corrections modify the size of the QCD-induced ALP potential. At very high temperatures above QCD confinement, the ALP potential is expected to behave as [109, 137–140]

$$V(a;T) = \chi(T)\left[1-\cos\left(\frac{a}{f_a'}\right)\right] = \chi_0\left(\frac{T}{150\,\mathrm{MeV}}\right)^{-n}\left[1-\cos\left(\frac{a}{f_a'}\right)\right], \tag{3.5}$$

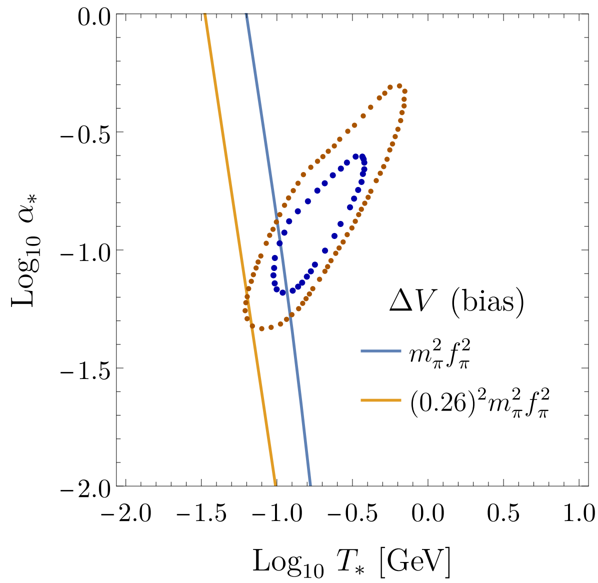

Figure 1. One and two sigma contours for the DW interpretation of the signal as provided by the [1] collaboration (blue and yellow dots). The prediction of a DW network with QCD induced bias ($\Delta V \sim \epsilon^2 m_\pi^2 f_\pi^2$) are displayed as lines with varying DW tension.

with $n \simeq 7$ and $\chi_0^{1/4} \simeq 75.6\,\mathrm{MeV}$, even though some uncertainty on these parameter still remains (see e.g. [140] and references therein). Similarly to the low-temperature case, some approximate alignment between QCD and the dark-QCD can lead to a parametric suppression of the natural bias $|\Delta V_k|(T) \sim \chi(T)$ to

$$|\Delta V_k|(T) \sim \epsilon^2 \chi(T)\,. \tag{3.6}$$

In our analysis we consider as a bias eq. (3.4) for $T \lesssim 150\,\mathrm{MeV}$ and eq. (3.6) for $T \gtrsim 150\,\mathrm{MeV}$.

From this simple estimate we can already draw some conclusions in the light of the recent PTA results. In ref. [1], the collaboration has performed a bayesian analysis on the NANOGrav data for the DW interpretation. The results were displayed in a two dimensional plane of T_* vs α_* as 1 and 2 sigma contours, as shown in figure 1, for the case of DWs as the only source contributing to the GW signal.

In order to compare the NANOGrav contours with the scenario we are discussing, we can first use equations (2.8) and (2.9) to relate directly the fraction of energy density to the annihilation temperature, for a given bias potential,

$$\alpha_* \simeq 0.15 \left(\frac{\Delta V^{1/4}}{100\,\mathrm{MeV}}\right)^4 \left(\frac{T_*}{100\,\mathrm{MeV}}\right)^{-4} \left(\frac{g_*}{10}\right)^{-1}. \tag{3.7}$$

Plugging in $\Delta V \sim \epsilon^2 m_\pi^2 f_\pi^2$ in the equation above we obtain a line in the T_* vs α_* plane.[8] Notice that each point on this line corresponds to a specific domain wall tension.

[8]In the region relevant for NANOGrav the network annihilates below $T = 150\,\mathrm{MeV}$ in our model, so that it is consistent to use the temperature independent potential (3.4).

We display in figure 1 the lines of two representative cases for ϵ, showing how the QCD-induced bias can accommodate the NANOGrav data. Notice that since $\epsilon \leq 1$ in this minimal realization, we cannot access the entire region favoured by the NANOGrav analysis in this model.

The results from the NANOGrav collaboration are obtained in a model-independent way assuming that the DW network is in the scaling regime at annihilation. In the following section, we shall investigate whether this assumption is compatible with the natural QCD bias.

4 The impact of friction from QCD

In this section we study the friction acting on the ALP domain wall as a consequence of the reflection of particles in the plasma. In particular, we are interested in friction effects close to the annihilation temperature of the network in the range relevant for figure 1. If friction dominates before annihilation, the DW network is not in scaling and the predictions for the GW spectrum can change significantly [71, 104], possibly jeopardizing the PTA interpretation. The irreducible friction on ALP domain walls in scenarios with the QCD bias comes from gluons and in general from hadrons at low temperatures.

The effect of friction is usually parameterized by defining a friction length ℓ_f which feeds in the total damping scale of the network ℓ_d as

$$\frac{1}{\ell_d} = 3H + \frac{1}{\ell_f}, \tag{4.1}$$

where H is the Hubble parameter and

$$\frac{1}{\ell_f} = \frac{\Delta P}{v_w \sigma_{\rm DW}}. \tag{4.2}$$

Here v_w is the average velocity of the network, and ΔP is the pressure on the wall from interactions with the plasma. The definition above takes into account that one generally expects $\Delta P \propto v_w$, at least for moderate velocities.

The pressure can be computed from an integral over the particle thermal distribution involving the reflection coefficient [71, 141], $\mathcal{R}(p_z)$,

$$\Delta P = \frac{2g}{(2\pi)^2} \int_0^\infty \mathrm{d}p_z p_z^2 \mathcal{R}(p_z) \frac{1}{\beta\gamma a} \left[2\beta\gamma p_z v_w - \log\left(\frac{f(-v_w)}{f(v_w)} \right) \right] \Big|_{E=\sqrt{p_z^2+m^2}}, \tag{4.3}$$

where $\gamma = \sqrt{1-v_w^2}$, $a = \pm 1$ for FD or BE statistics respectively, p_z is the particle momentum in the direction orthogonal to the wall, β is the inverse temperature, g counts the number of d.o.f, and $f(v)$ is the thermal distribution in the wall rest frame

$$f(v) = \frac{g}{e^{\gamma(v)\beta(E+p_z v)} \pm 1}. \tag{4.4}$$

The reflection coefficient $\mathcal{R}(p_z)$ can be computed by solving the quantum mechanical reflection for a particle scattering off the ALP wall. For temperatures such that $1/\ell_f \gtrsim 3H$

JHEP11(2023)169

the DW network deviates from scaling and enters a friction dominated regime, where one expects suppressed GW signals [71, 104]. Indeed, by considering only the velocity one-scale (VOS) estimate as done in ref. [71], the GW signal would be suppressed by a factor v_w^5, showing that it is unlikely we could explain the large amplitude seen at PTAs.

The temperatures of interest for PTA are in the ballpark of the QCD crossover, making the computation of the friction from QCD effects rather difficult. We face this issue following a very minimal strategy,[9] and we study two regimes of temperatures above and below the QCD scale:

- For $T \gtrsim 2\,\text{GeV}$ we compute friction by considering the scattering of gluons off the ALP DW through the interaction (3.1).
- For $T \lesssim 60\,\text{MeV}$ we employ chiral perturbation theory, and the main source of friction is induced by scattering of pions off the ALP DW.

Even if we cannot compute the friction in the intermediate temperature regime, we will still be able to draw interesting conclusions concerning the DW dynamics around the QCD crossover.

4.1 Friction from gluons

At high temperatures, the contribution to ΔP comes from gluons reflecting off the ALP domain wall. We stress that this effect is unavoidable in the scenario in which QCD provides the bias collapsing the network.

In the simplified picture of friction as coming from one-to-one particle reflection off the ALP wall, we can neglect as a first approximation the gluon self interactions and work at the linear order in the field fluctuations. In this limit, one recovers independent abelian equations of motion for each gluon degree of freedom. Additionally, when the ALP wall comes from the simplest cosine potential, a reasonable approximation for the reflection coefficient can be obtained analytically [144] (see also [105]). The reflection probability for a negative helicity gluon is given by

$$R^-(\rho) = \frac{1 + \cos(\pi\sqrt{1+b\rho})}{\cos(\pi\sqrt{1+b\rho}) + \cosh(4\pi\rho)}, \tag{4.5}$$

where $\rho = p_z/m_a$, with p_z the gluon momentum in the direction orthogonal to the wall, and

$$b = \frac{4N_c}{\pi N_d}\alpha_s. \tag{4.6}$$

The reflection for positive helicity gives a quantitatively very similar result as in (4.5) in the case of interest. At momenta much below the inverse width of the domain wall, $\rho \ll 1$, particles have a finite probability of being reflected $\propto b^2$.

[9] This should be seen as a first approximation to the problem of hadrons scattering off axionic DWs. A more detailed analysis, for instance along the lines used for thermal axion production in [142, 143], is left for future work.

The pressure induced by this type of interaction may be computed according to (4.3) and grows with the temperature as

$$\Delta P = v_w \, g \frac{3}{32\pi^2} b^2 T^4, \quad T \ll m_a, \tag{4.7}$$

where $g = 2 \cdot 8$ for gluons. For temperatures $T \gtrsim m_a$ an even larger fraction of particles is simply transmitted and the $\propto T^4$ behavior is tamed to a much slower increase $\propto T$,

$$\Delta P = 2 \cdot 10^{-5} \cdot v_w \, g \, b^2 m_a^3 T, \quad T \gg m_a. \tag{4.8}$$

Our calculation of the friction at low temperatures is of course limited by QCD becoming non-perturbative. In our analysis we will push this description down to $T \gtrsim 2\,\text{GeV}$, keeping in mind that corrections should be expected at the low end of this region.

Notice also that there is a source of model dependence given by the ratio of the QCD and dark-QCD anomaly, N_c/N_d. Clearly, when $N_c \to 0$ the ALP is decoupled from QCD and indeed (4.7) and (4.8) yield a vanishing contribution. In the following we shall take $N_c/N_d = \mathcal{O}(1)$, as decoupling the ALP from QCD is anyway not compatible with the generation of the required bias term.

Let us finally notice that the pressure from gluon reflection is generally much bigger than the high-temperature bias induced by the QCD instantons in (3.6). This crucially implies that the network can consistently reach a friction-dominated regime well before annihilation begins.

4.2 Friction from pions

In order to evaluate the friction from pions we refer to chiral perturbation theory and consider the potential in (3.2). Let us first notice that in the scenario of interest where the QCD contribution is not aligned with the potential induced by the dark QCD, the pion mass will change in the different vacua. This simply signals that the $\mathbb{Z}_{N_{\rm DW}}$ degeneracy has in fact been removed by the QCD potential. Taking this into account, the pressure from the pions is expected to be the same order of the potential bias.

This pressure is however not what we are interested in, as it would only determine the velocity of the domain walls during the collapse, very similarly to the case of a first order phase transition (see e.g. [141]). Instead, the question we wish to address is whether the ALP interaction with pions could in principle turn a scaling network (where the bias is by definition irrelevant) into a friction-dominated evolution.

We shall then evaluate the pion pressure in a system in which the QCD potential and the dark-QCD potential are chosen to be aligned. This ensures that the pressure we are evaluating receives no contribution from the bias term (which is vanishing due to the alignment), and it can therefore be interpreted as the friction that would be acting on scaling domain walls. The only contribution comes then from pion reflection, with the pion mass being the same on both sides of the ALP wall. This can also be seen as a lower bound on the actual friction from hadrons.

We then set $f_a = f_a'$ only for this specific calculation to ensure the alignment, and we additionally assume a large hierarchy between the ALP and the pion mass, $m_a \gg m_\pi$.

This allows us to neglect the backreaction of the pion (and in general of the QCD sector) on the ALP domain wall solution (2.5), which is in fact obtained considering only the dark-QCD potential. In addition, this mass hierarchy allows us to neglect the effect of ALP excitations. We shall therefore treat the ALP field as a non-dynamical z-dependent background given by (2.5), and study the motion of the π_0 around it.

Firstly, one has to take into account that the ALP background induces a z-dependent background on the π_0 as well, given as the solution of

$$-\pi_b''(z) + \frac{\partial V(a(z),\pi_0)}{\partial \pi_0}\Big|_{\pi_0=\pi_b(z)} = 0. \tag{4.9}$$

The boundary conditions for $\pi_b(z)$ at $z = \pm\infty$ can be derived from the structure of the vacua in eq. (3.2), considering that $a(-\infty) = 0$ and $a(+\infty)/f_a = 2\pi$. One then finds:

$$\pi_b(-\infty)/f_\pi = 0, \quad \pi_b(+\infty)/f_\pi = -\pi. \tag{4.10}$$

According to the assumed hierarchy $m_a \gg m_\pi$, the ALP background varies on scales much shorter than the inverse pion mass. We can therefore set $a(z<0) = a(-\infty)$ and similarly for positive z, and split eq. (4.9) on the two sides of the ALP wall as

$$\begin{cases} -\frac{\pi_b^{-\,\prime\prime}(z)}{f_\pi} + m_\pi^2 \sin\left(\frac{\pi_b^-(z)}{f_\pi}\right) = 0 & z<0, \\ -\frac{\pi_b^{+\,\prime\prime}(z)}{f_\pi} - m_\pi^2 \sin\left(\frac{\pi_b^+(z)}{f_\pi}\right) = 0 & z>0. \end{cases} \tag{4.11}$$

Once the solution $\pi_b^-(z)$ is obtained, $\pi_b^+(z)$ is simply given by $\pi_b^+(z) = -\pi f_\pi + \pi_b^-(-z)$.

The equations of motion for $\pi_b(z)$ are similar to the ones of the sine-Gordon model but they are not quite the same, given that sine-Gordon potential would be $\propto \cos(\pi_0/f_\pi)$ for both positive and negative z. This, together with the different boundary conditions of the present case, implies that contrary to the sine-Gordon model, where particle excitations are exactly (self) reflectionless, pions can have a non-zero reflection coefficient.

The profile $\pi_b(z)$ can be obtained by solving numerically the equation of motion. To this end we employ a relaxation algorithm taking the ALP profile to be a step function as in (4.11), as well as considering the realistic ALP solution (2.5) with $m_\pi/m_a = 0.1$. We find that, as long as the ALP mass is hierarchically larger than m_π, the solution for $\pi_b(z)$ is practically independent of m_a. Qualitatively, one has

$$\pi_b(z)/f_\pi \sim -2\arctan\left(e^{m_\pi z}\right), \quad m_\pi \ll m_a, \tag{4.12}$$

even though corrections are clearly visible in figure 2 (left panel), as (4.12) does not in fact solve the equation of motion. Notice that the resulting ALP-π_0 domain wall has structure at two different scales, m_a^{-1} and m_π^{-1}, similarly to the case of η'–π_0 domain walls in pure QCD [145].

As a cross check, we have used the same relaxation algorithm to the full ALP-π_0 potential including (2.4) and (3.2), thus taking into account the QCD contribution to the ALP domain wall modifying the shape in (2.5). The resulting profiles for the ALP and the

JHEP11(2023)169

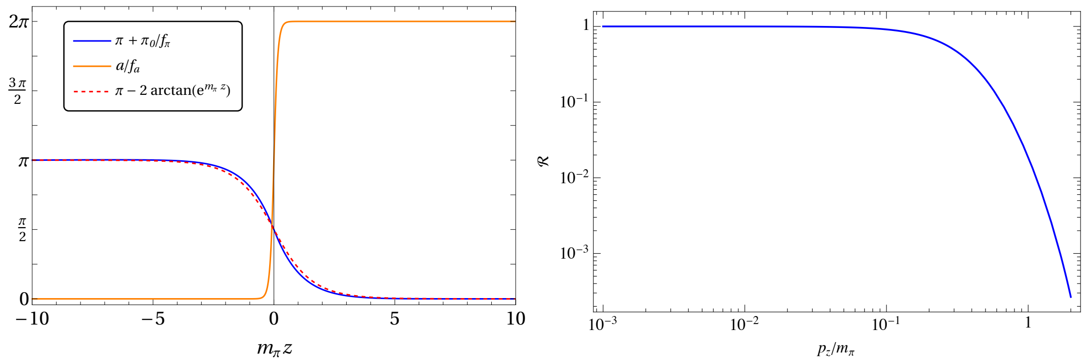

Figure 2. *Left*: results for the pion profile $\pi_b(z)$ (blue) in the presence of a realistic ALP background (orange) as given in (2.5) with $m_\pi/m_a = 0.1$ obtained numerically with a relaxation algorithm. The dashed red line shows the qualitative behavior discussed in the text. The pion profile varies on a scale $\sim m_\pi^{-1}$ much larger than the ALP background $\sim m_a^{-1}$. *Right*: reflection probability for the pion self-scattering as a function of the incoming momentum.

π_0 agree very well with the solution of the simplified one-field problem in (4.11) (shown in figure 2), confirming the intuition that for a heavy ALP the pion backreaction can be safely neglected.

Given our background solution for the pion field, we can calculate the reflection probability for particle fluctuations around it. We will follow a similar strategy as the one employed to evaluate the pion background in the presence of the ALP profile and consider the pion as the only dynamical field, given our assumption that $m_\pi \ll m_a$. Writing $\pi_0 = \pi_b(z) + \delta\pi_0(x)$, and $\delta\pi_0(x) = f(z)e^{iEt-ik_x x-ik_y y}$, we obtain the following equation of motion:

$$f''(z) + \left[k_z^2 + m_\pi^2 - \frac{\partial^2 V}{\partial \pi_0^2}(a(z), \pi_b(z))\right] f(z) = 0. \tag{4.13}$$

Notice that the second derivative of the potential equals m_π^2 at $z = -\infty$, so that the incoming particle is described by a plane wave.

The reflection coefficient is evaluated by solving (4.13) numerically, and the result is shown in the right panel of figure 2. Similarly to the previous discussion, the reflection probability is practically unchanged when moving from the step-function approximation for $a(z)$ to a realistic profile as long as $m_\pi \ll m_a$. For large incoming momenta $p_z \gtrsim m_\pi$, we are able to identify an exponential drop in the reflection probability, as expected when the momentum of the scattering particle is of the same order of the inverse wall width $\sim m_\pi^{-1}$. Notice however that this kinematic region is not particularly relevant for our analysis, as we apply the pion Lagrangian only at temperatures $T \lesssim 60\,\text{MeV}$, where high-momentum excitations are Boltzmann suppressed.

Using our numerical result for the reflection coefficient and (4.3), we can straightforwardly evaluate the pressure from pion reflection in the alignment limit under consideration. The resulting pressure is approximated by the following analytical expression:

$$\Delta P_\pi \sim 10^{-3} \cdot v_w\, g_\pi\, m_\pi^3\, T\, e^{-m_\pi/T}, \quad T < m_\pi \ll m_a, \tag{4.14}$$

where we have included $g_\pi = 3$ expecting a similar contribution from the charged pions as well. When presenting our results in section 5, we will nevertheless use the full numerical result instead of (4.14).

5 Implications of friction for PTAs

In this final section we summarize our results by indicating the ALP parameter space where deviations from the scaling regime of the DW network are to be expected at temperatures around annihilation, thus possibly affecting the corresponding SGWB.

For temperatures $60\,\text{MeV} < T < 2\,\text{GeV}$ the pressure from the hadronic sector is not calculable within our simple approach. However, to gain information on this intermediate temperature range we can look at the pressure at higher temperatures above $2\,\text{GeV}$ (from gluons) and at lower temperatures below $60\,\text{MeV}$ (from pions). Notice that for $T < 60\,\text{MeV}$ we consider the pressure from pions that would be acting on the ALP domain walls as if annihilation had not happened. In practice, the NANOGrav data suggests annihilation temperatures $T_* > 60\,\text{MeV}$ for our model with the QCD bias, so that the would-be pion pressure is only useful for the purpose of the extrapolation in the intermediate range.

In particular, if both the gluon and the would-be pion pressure were to dominate in their temperature range of validity, we would conclude that annihilation at some intermediate temperature is very likely to occur during friction domination. On the other hand, if friction dominates in only one of the two calculable temperature regimes, a more detailed analysis around the QCD crossover is needed to determine whether annihilation occurs or not in the scaling regime.

We now illustrate this strategy by presenting in figure 3 two benchmark points characterized by representative choices of the model parameters. The left panel shows a benchmark for which the signal from scaling domain walls and QCD-induced bias can explain the PTA data, indicated by $\alpha_* = \alpha_{\text{obs}}$. As we can see, the network does actually enter friction domination around $T \sim 100\,\text{GeV}$, driven by gluon scattering. Friction remains dominant also at $T \sim 2\,\text{GeV}$, which we take as the edge for the validity of the gluon calculation. However, at temperatures $T \sim 60\,\text{MeV}$ the would-be pressure from the pions is insufficient to drive the DW network away from scaling. Therefore, it is possible that the period of friction domination ends somewhere inside the gray region where neither of our calculation is applicable, and the DW network goes back to scaling just before annihilation, which in this benchmark is predicted around $T_{\text{ann}} \sim 65\,\text{MeV}$. Points of this type are shown in figure 4 in the purple region labelled as "gluon friction", where we suggest that a more refined analysis is needed in order to establish their viability to explain the PTA signal.[10]

In the right panel of figure 3 we show instead a benchmark point for which the gluon and would-be pion pressure are both satisfying the friction domination condition in their relevant temperature range. In this case, it is very likely that the domain walls collapse without ever going back to the scaling regime, with strong implications for the emitted GWs. However, points of this kind where friction dominates in both our calculable regions

[10] In fact, even if plasma effects become unimportant for $T > T_{\text{ann}}$, the network will still take a finite time to go back to the scaling regime.

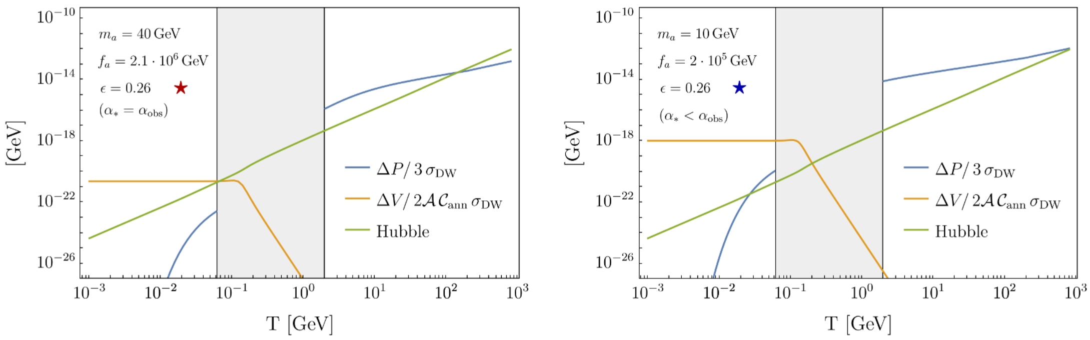

Figure 3. Benchmark points illustrating our friction-domination analysis. *Left*: friction domination starts at temperatures $T \sim 100\,\text{GeV}$ due to the gluon scattering, as the properly normalized pressure (blue line) overcomes Hubble (green line). At lower temperature, the would-be pion pressure is however unable to drive friction domination. Whether the network will have enough time to go back to scaling at $T_{\rm ann}$ remains uncertain. If this is the case, this benchmark point can explain the PTA signal ($\alpha_* = \alpha_{\rm obs}$). *Right*: gluon and would-be pion pressure are both capable of inducing friction domination, and thus it is very likely that the network never goes back to scaling above the annihilation temperature, identified as the crossing between the properly normalized bias (orange line) and Hubble. Points of this kind, however, require a relatively small domain wall tension and would not be able to explain the PTA signal, even if they were to annihilate in the scaling regime ($\alpha_* < \alpha_{\rm obs}$). The anomaly coefficients have been chosen as $N_c/N_d = 3/2$.

require a relatively small tension, and therefore cannot explain the GW signal observed at PTAs, even if the network were to annihilate in the scaling regime (emphasized in the right panel of figure 3 as $\alpha_* < \alpha_{\rm obs}$). Points of this kind are found in the "pion and gluon friction" region in figure 4.

Let us now comment on our overall results shown in figure 4 as a scan over the (m_a, f_a) parameter space. Additionally to the regions mentioned in the previous paragraphs, we see that there exists parameter space for $m_a < 2\,\text{GeV}$ where only the would-be pion friction is able to induce friction domination, while gluons do not. This is understood by noticing that the gluon reflection becomes more and more suppressed as m_a is lowered, see e.g. eq. (4.7). On the other hand, as long as $m_a \gg m_\pi$ the would-be pion pressure is independent of m_a. This, combined with the fact that gluons need to face a faster Hubble expansion at higher temperatures, leads to the "only pion friction" region in figure 4. Notice also that our scan does not extend to points with $m_a < 1\,\text{GeV}$ as the approximation $m_a \gg m_\pi$ used in section 4.2 would break down.

Together with the colored regions indicating the impact of friction, we also show in (dark) gray the parameter space where domain walls come to dominate the energy of the Universe before annihilation for the choice $\epsilon = 0.26$ ($\epsilon = 1$) for the bias in eq. (3.4).

The parameter space that can fit the NANOGrav data assuming that the network annihilates during the scaling regime is shown by the light blue band for $\epsilon = 1$ and by the narrower orange band for $\epsilon = 0.26$. These signal bands follow straightforwardly from the results shown in figure 1. As we can see, both these regions are not too far from domain

JHEP11(2023)169

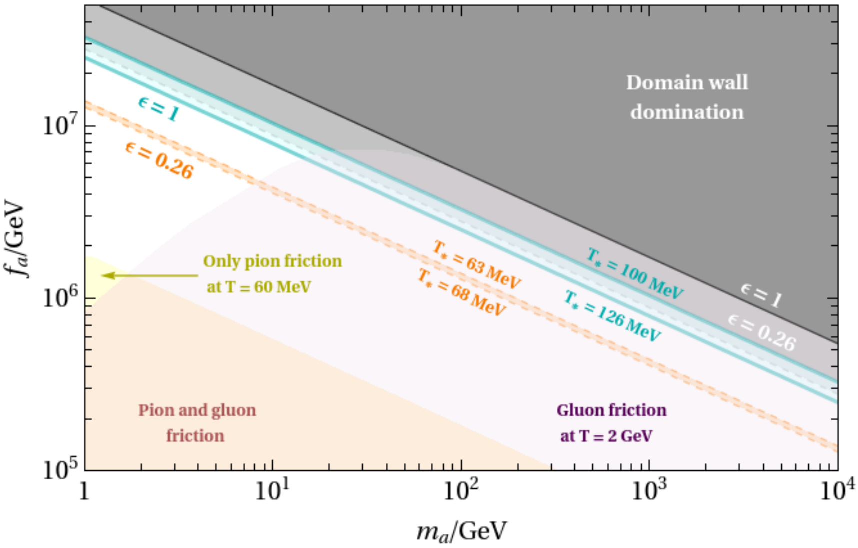

Figure 4. Scan over the (m_a, f_a) parameter space summarizing the results of our analysis. The light blue (orange) band indicates the parameter space that is compatible with the NANOGrav data in the ALP model with a QCD bias considered here with $\epsilon = 1$ ($\epsilon = 0.26$), for which the annihilation temperature range is $T_* = [100 - 126]\,\text{MeV}$ ($T_* = [63 - 68]\,\text{MeV}$). As the observed GW background is rather large, both our signal bands are not too far from domain wall domination, shown in the upper right corner by the dark gray (gray) region for $\epsilon = 1$ ($\epsilon = 0.26$). The other colored regions highlight the relevance of friction. The purple region corresponds to the parameter space where gluon friction dominates over Hubble at $T = 2\,\text{GeV}$, where we take $\alpha_s = 0.2$ and $N_c/N_d = 3/2$. This is the lowest temperature where the gluon computation can be trusted, see also figure 3. The would-be pion pressure is evaluated at $T = 60\,\text{MeV}$ and provides information about friction in the confined phase, see text for details. The region where the would-be pion pressure can induce friction domination is shown in yellow, and its intersection with the gluon friction region is shown by the orange color. The implication for the ALP domain wall interpretation of the PTA data is as follows: for relatively light ALPs with $m_a < 10\,\text{GeV}$ it is fair to assume that the network annihilates in the scaling regime, so that the signal bands shown here can indeed explain the NANOGrav data. On the other hand, for $m_a > 10\,\text{GeV}$ friction is shown to be important at least to the right of the QCD crossover, and a more detailed analysis is required to assess the viability of this interpretation. The red and blue stars correspond to the benchmark points shown in figure 3.

wall domination. This is expected given that the preferred values for the (normalized) network energy density at annihilation are rather large, $\alpha_\star \sim 0.1$.

The intersection of these signal bands and our friction regions provides the main result of our analysis, which we now summarize. Most of the parameter space compatible with the NANOGrav data implies friction domination from gluons at high temperatures. However, the would-be pion pressure at low temperatures is not big enough to conclude that the network will be friction dominated at annihilation as well. We nevertheless suggest that a more detailed analysis is needed to ensure viability of these points. On the other hand, for a relatively light ALP with $m_a < 10\,\text{GeV}$ we find no evidence for friction domination around the QCD crossover, and thus these regions of parameter space can be viable candidates to

JHEP11(2023)169

explain the PTA data. Even though our analysis cannot extend for $m_a < 1\,\mathrm{GeV}$, we expect this conclusion to apply also for lighter ALPs.

Before concluding this section, let us mention again that our results only take into account the inevitable friction on the DW network in scenarios with a QCD bias, and that additional, although model-dependent, interactions with the other SM particles can provide important sources of friction as well (see [71]).

6 Conclusions

The results from PTAs have opened a new era of exploration of the Universe by providing the first evidence of a stochastic background of gravitational waves. One possible cosmological explanation for this signal is a network of DWs annihilating around the temperature of the QCD crossover.

An important class of DWs arising in BSM theories is the one connected to models including ALPs. Moreover, as the data suggest annihilation temperatures around the QCD crossover, it is very natural to consider the case in which the bias annihilating the DW network comes in fact from the anomalous ALP-gluon coupling, contributing to the ALP potential precisely around the QCD confinement. Considering the standard prediction for the SGWB produced by DWs in the scaling regime, this natural scenario is indeed capable of explaining the signal observed at PTAs.

However, any deviation from scaling, e.g. due to particle friction, can affect the GW signal from DWs and therefore the viability of this interpretation. Our main observation in this regard is that the natural scenario where annihilation is induced by QCD comes with an unavoidable source of friction exerted by hadronic states scattering off the ALP DWs, and it is therefore important to take this effect into account.

Our results are summarized in figure 4, where we have identified the portion of the ALP parameter space where friction can be relevant, even though for values of the domain wall tension that are capable of explaining the NANOGrav data we cannot firmly conclude whether friction will be dominant at the annihilation temperature. This is mainly because of the lack of calculability around the QCD crossover within our simplified approach, and a more refined analysis would be required. On the other hand, we have identified the region of ALP parameter space corresponding to $m_a \lesssim 10\,\mathrm{GeV}$ where friction is negligible and the ALP DW interpretation of the NANOGrav signal is unaffected by particle friction.

Acknowledgments

All authors are supported in part by the Strategic Research Program High-Energy Physics of the Research Council of the Vrije Universiteit Brussel and by the iBOF "Unlocking the Dark Universe with Gravitational Wave Observations: from Quantum Optics to Quantum Gravity" of the Vlaamse Interuniversitaire Raad. SB and AM are supported in part by the "Excellence of Science — EOS" — be.h project n.30820817, and by the FWO-NSFC samenwerkingsproject VS02223N. SB and AR are supported by FWO-Vlaanderen through grant numbers 12B2323N and 1152923N respectively. AS is supported in part by the FWO-Vlaanderen through the project G006119N.

References

[1] NANOGrav collaboration, *The NANOGrav 15 yr Data Set: Search for Signals from New Physics*, *Astrophys. J. Lett.* **951** (2023) L11 [arXiv:2306.16219] [INSPIRE].

[2] NANOGrav collaboration, *The NANOGrav 15 yr Data Set: Observations and Timing of 68 Millisecond Pulsars*, *Astrophys. J. Lett.* **951** (2023) L9 [arXiv:2306.16217] [INSPIRE].

[3] NANOGrav collaboration, *The NANOGrav 15 yr Data Set: Evidence for a Gravitational-wave Background*, *Astrophys. J. Lett.* **951** (2023) L8 [arXiv:2306.16213] [INSPIRE].

[4] EPTA collaboration, *The second data release from the European Pulsar Timing Array. I. The dataset and timing analysis*, *Astron. Astrophys.* **678** (2023) A48 [arXiv:2306.16224] [INSPIRE].

[5] EPTA, InPTA: collaboration, *The second data release from the European Pulsar Timing Array. III. Search for gravitational wave signals*, *Astron. Astrophys.* **678** (2023) A50 [arXiv:2306.16214] [INSPIRE].

[6] European Pulsar Timing Array collaboration, *Second Data Release from the European Pulsar Timing Array. VI. Challenging the Ultralight Dark Matter Paradigm*, *Phys. Rev. Lett.* **131** (2023) 171001 [arXiv:2306.16228] [INSPIRE].

[7] A. Zic et al., *The Parkes Pulsar Timing Array Third Data Release*, arXiv:2306.16230 [INSPIRE].

[8] D.J. Reardon et al., *Search for an Isotropic Gravitational-wave Background with the Parkes Pulsar Timing Array*, *Astrophys. J. Lett.* **951** (2023) L6 [arXiv:2306.16215] [INSPIRE].

[9] H. Xu et al., *Searching for the Nano-Hertz Stochastic Gravitational Wave Background with the Chinese Pulsar Timing Array Data Release I*, *Res. Astron. Astrophys.* **23** (2023) 075024 [arXiv:2306.16216] [INSPIRE].

[10] B.B.P. Perera et al., *The International Pulsar Timing Array: Second data release*, *Mon. Not. Roy. Astron. Soc.* **490** (2019) 4666 [arXiv:1909.04534] [INSPIRE].

[11] J. Antoniadis et al., *The International Pulsar Timing Array second data release: Search for an isotropic gravitational wave background*, *Mon. Not. Roy. Astron. Soc.* **510** (2022) 4873 [arXiv:2201.03980] [INSPIRE].

[12] NANOGrav collaboration, *The NANOGrav 12.5 yr Data Set: Search for an Isotropic Stochastic Gravitational-wave Background*, *Astrophys. J. Lett.* **905** (2020) L34 [arXiv:2009.04496] [INSPIRE].

[13] EPTA collaboration, *Common-red-signal analysis with 24-yr high-precision timing of the European Pulsar Timing Array: inferences in the stochastic gravitational-wave background search*, *Mon. Not. Roy. Astron. Soc.* **508** (2021) 4970 [arXiv:2110.13184] [INSPIRE].

[14] B. Goncharov et al., *On the Evidence for a Common-spectrum Process in the Search for the Nanohertz Gravitational-wave Background with the Parkes Pulsar Timing Array*, *Astrophys. J. Lett.* **917** (2021) L19 [arXiv:2107.12112] [INSPIRE].

JHEP11(2023)169

[15] S. Burke-Spolaor et al., *The Astrophysics of Nanohertz Gravitational Waves*, *Astron. Astrophys. Rev.* **27** (2019) 5 [arXiv:1811.08826] [INSPIRE].

[16] C. Han, K.-P. Xie, J.M. Yang and M. Zhang, *Self-interacting dark matter implied by nano-Hertz gravitational waves*, arXiv:2306.16966 [INSPIRE].

[17] S.-Y. Guo, M. Khlopov, X. Liu, L. Wu, Y. Wu and B. Zhu, *Footprints of Axion-Like Particle in Pulsar Timing Array Data and JWST Observations*, arXiv:2306.17022 [INSPIRE].

[18] E. Megias, G. Nardini and M. Quiros, *Pulsar timing array stochastic background from light Kaluza-Klein resonances*, *Phys. Rev. D* **108** (2023) 095017 [arXiv:2306.17071] [INSPIRE].

[19] K. Fujikura, S. Girmohanta, Y. Nakai and M. Suzuki, *NANOGrav signal from a dark conformal phase transition*, *Phys. Lett. B* **846** (2023) 138203 [arXiv:2306.17086] [INSPIRE].

[20] J. Yang, N. Xie and F.P. Huang, *Implication of nano-Hertz stochastic gravitational wave background on ultralight axion particles*, arXiv:2306.17113 [INSPIRE].

[21] N. Kitajima, J. Lee, K. Murai, F. Takahashi and W. Yin, *Gravitational Waves from Domain Wall Collapse, and Application to Nanohertz Signals with QCD-coupled Axions*, arXiv:2306.17146 [INSPIRE].

[22] Y. Bai, T.-K. Chen and M. Korwar, *QCD-Collapsed Domain Walls: QCD Phase Transition and Gravitational Wave Spectroscopy*, arXiv:2306.17160 [INSPIRE].

[23] L. Zu, C. Zhang, Y.-Y. Li, Y.-C. Gu, Y.-L.S. Tsai and Y.-Z. Fan, *Mirror QCD phase transition as the origin of the nanohertz Stochastic Gravitational-Wave Background*, arXiv:2306.16769 [INSPIRE].

[24] S. Vagnozzi, *Inflationary interpretation of the stochastic gravitational wave background signal detected by pulsar timing array experiments*, *JHEAp* **39** (2023) 81 [arXiv:2306.16912] [INSPIRE].

[25] G. Lambiase, L. Mastrototaro and L. Visinelli, *Astrophysical neutrino oscillations after pulsar timing array analyses*, arXiv:2306.16977 [INSPIRE].

[26] J. Ellis et al., *Gravitational Waves from SMBH Binaries in Light of the NANOGrav 15-Year Data*, arXiv:2306.17021 [INSPIRE].

[27] Y.-Y. Li et al., *Primordial magnetic field as a common solution of nanohertz gravitational waves and Hubble tension*, arXiv:2306.17124 [INSPIRE].

[28] G. Franciolini, D. Racco and F. Rompineve, *Footprints of the QCD Crossover on Cosmological Gravitational Waves at Pulsar Timing Arrays*, arXiv:2306.17136 [INSPIRE].

[29] Z.-Q. Shen, G.-W. Yuan, Y.-Y. Wang and Y.-Z. Wang, *Dark Matter Spike surrounding Supermassive Black Holes Binary and the nanohertz Stochastic Gravitational Wave Background*, arXiv:2306.17143 [INSPIRE].

[30] J. Ellis, M. Lewicki, C. Lin and V. Vaskonen, *Cosmic superstrings revisited in light of NANOGrav 15-year data*, *Phys. Rev. D* **108** (2023) 103511 [arXiv:2306.17147] [INSPIRE].

[31] G. Franciolini, A. Iovino, Junior., V. Vaskonen and H. Veermae, *Recent Gravitational Wave Observation by Pulsar Timing Arrays and Primordial Black Holes: The Importance of Non-Gaussianities*, *Phys. Rev. Lett.* **131** (2023) 201401 [arXiv:2306.17149] [INSPIRE].

JHEP11(2023)169

[32] Z. Wang, L. Lei, H. Jiao, L. Feng and Y.-Z. Fan, *The nanohertz stochastic gravitational wave background from cosmic string loops and the abundant high redshift massive galaxies*, *Sci. China Phys. Mech. Astron.* **66** (2023) 120403 [arXiv:2306.17150] [INSPIRE].

[33] A. Ghoshal and A. Strumia, *Probing the Dark Matter density with gravitational waves from super-massive binary black holes*, arXiv:2306.17158 [INSPIRE].

[34] S. Blasi, V. Brdar and K. Schmitz, *Has NANOGrav found first evidence for cosmic strings?*, *Phys. Rev. Lett.* **126** (2021) 041305 [arXiv:2009.06607] [INSPIRE].

[35] J. Ellis and M. Lewicki, *Cosmic String Interpretation of NANOGrav Pulsar Timing Data*, *Phys. Rev. Lett.* **126** (2021) 041304 [arXiv:2009.06555] [INSPIRE].

[36] W. Buchmuller, V. Domcke and K. Schmitz, *From NANOGrav to LIGO with metastable cosmic strings*, *Phys. Lett. B* **811** (2020) 135914 [arXiv:2009.10649] [INSPIRE].

[37] L. Bian, R.-G. Cai, J. Liu, X.-Y. Yang and R. Zhou, *Evidence for different gravitational-wave sources in the NANOGrav dataset*, *Phys. Rev. D* **103** (2021) L081301 [arXiv:2009.13893] [INSPIRE].

[38] S. Vagnozzi, *Implications of the NANOGrav results for inflation*, *Mon. Not. Roy. Astron. Soc.* **502** (2021) L11 [arXiv:2009.13432] [INSPIRE].

[39] Z.-C. Chen, C. Yuan and Q.-G. Huang, *Pulsar Timing Array Constraints on Primordial Black Holes with NANOGrav 11-Year Dataset*, *Phys. Rev. Lett.* **124** (2020) 251101 [arXiv:1910.12239] [INSPIRE].

[40] C.-W. Chiang and B.-Q. Lu, *Testing clockwork axion with gravitational waves*, *JCAP* **05** (2021) 049 [arXiv:2012.14071] [INSPIRE].

[41] M. Benetti, L.L. Graef and S. Vagnozzi, *Primordial gravitational waves from NANOGrav: A broken power-law approach*, *Phys. Rev. D* **105** (2022) 043520 [arXiv:2111.04758] [INSPIRE].

[42] J.J. Blanco-Pillado, K.D. Olum and J.M. Wachter, *Comparison of cosmic string and superstring models to NANOGrav 12.5-year results*, *Phys. Rev. D* **103** (2021) 103512 [arXiv:2102.08194] [INSPIRE].

[43] A.S. Sakharov, Y.N. Eroshenko and S.G. Rubin, *Looking at the NANOGrav signal through the anthropic window of axionlike particles*, *Phys. Rev. D* **104** (2021) 043005 [arXiv:2104.08750] [INSPIRE].

[44] L. Bian, J. Shu, B. Wang, Q. Yuan and J. Zong, *Searching for cosmic string induced stochastic gravitational wave background with the Parkes Pulsar Timing Array*, *Phys. Rev. D* **106** (2022) L101301 [arXiv:2205.07293] [INSPIRE].

[45] Z.-C. Chen, Y.-M. Wu and Q.-G. Huang, *Search for the Gravitational-wave Background from Cosmic Strings with the Parkes Pulsar Timing Array Second Data Release*, *Astrophys. J.* **936** (2022) 20 [arXiv:2205.07194] [INSPIRE].

[46] D. Wang, *Novel Physics with International Pulsar Timing Array: Axionlike Particles, Domain Walls and Cosmic Strings*, arXiv:2203.10959 [INSPIRE].

[47] R.Z. Ferreira, A. Notari, O. Pujolas and F. Rompineve, *Gravitational waves from domain walls in Pulsar Timing Array datasets*, *JCAP* **02** (2023) 001 [arXiv:2204.04228] [INSPIRE].

[48] N. Ramberg, W. Ratzinger and P. Schwaller, *One μ to rule them all: CMB spectral distortions can probe domain walls, cosmic strings and low scale phase transitions*, *JCAP* **02** (2023) 039 [arXiv:2209.14313] [INSPIRE].

JHEP11(2023)169

[49] T. Bringmann, P.F. Depta, T. Konstandin, K. Schmidt-Hoberg and C. Tasillo, *Does NANOGrav observe a dark sector phase transition?*, JCAP **11** (2023) 053 [arXiv:2306.09411] [INSPIRE].

[50] E. Madge et al., *Primordial gravitational waves in the nano-Hertz regime and PTA data — towards solving the GW inverse problem*, JHEP **10** (2023) 171 [arXiv:2306.14856] [INSPIRE].

[51] T.W.B. Kibble, *Topology of Cosmic Domains and Strings*, J. Phys. A **9** (1976) 1387 [INSPIRE].

[52] Y.B. Zeldovich, I.Y. Kobzarev and L.B. Okun, *Cosmological Consequences of the Spontaneous Breakdown of Discrete Symmetry*, *Zh. Eksp. Teor. Fiz.* **67** (1974) 3 [INSPIRE].

[53] T. Higaki, K.S. Jeong, N. Kitajima, T. Sekiguchi and F. Takahashi, *Topological Defects and nano-Hz Gravitational Waves in Aligned Axion Models*, JHEP **08** (2016) 044 [arXiv:1606.05552] [INSPIRE].

[54] G.B. Gelmini, A. Simpson and E. Vitagliano, *Gravitational waves from axionlike particle cosmic string-wall networks*, Phys. Rev. D **104** (2021) 061301 [arXiv:2103.07625] [INSPIRE].

[55] G.B. Gelmini, S. Pascoli, E. Vitagliano and Y.-L. Zhou, *Gravitational wave signatures from discrete flavor symmetries*, JCAP **02** (2021) 032 [arXiv:2009.01903] [INSPIRE].

[56] G.B. Gelmini, A. Simpson and E. Vitagliano, *Catastrogenesis: DM, GWs, and PBHs from ALP string-wall networks*, JCAP **02** (2023) 031 [arXiv:2207.07126] [INSPIRE].

[57] N. Craig, I. Garcia Garcia, G. Koszegi and A. McCune, *P not PQ*, JHEP **09** (2021) 130 [arXiv:2012.13416] [INSPIRE].

[58] R. Zambujal Ferreira, A. Notari, O. Pujolàs and F. Rompineve, *High Quality QCD Axion at Gravitational Wave Observatories*, Phys. Rev. Lett. **128** (2022) 141101 [arXiv:2107.07542] [INSPIRE].

[59] E. Babichev, D. Gorbunov, S. Ramazanov and A. Vikman, *Gravitational shine of dark domain walls*, JCAP **04** (2022) 028 [arXiv:2112.12608] [INSPIRE].

[60] B. Barman, D. Borah, A. Dasgupta and A. Ghoshal, *Probing high scale Dirac leptogenesis via gravitational waves from domain walls*, Phys. Rev. D **106** (2022) 015007 [arXiv:2205.03422] [INSPIRE].

[61] Y. Wu, K.-P. Xie and Y.-L. Zhou, *Classification of Abelian domain walls*, Phys. Rev. D **106** (2022) 075019 [arXiv:2205.11529] [INSPIRE].

[62] D. Borah and A. Dasgupta, *Probing left-right symmetry via gravitational waves from domain walls*, Phys. Rev. D **106** (2022) 035016 [arXiv:2205.12220] [INSPIRE].

[63] Y. Wu, K.-P. Xie and Y.-L. Zhou, *Collapsing domain walls beyond Z_2*, Phys. Rev. D **105** (2022) 095013 [arXiv:2204.04374] [INSPIRE].

[64] B. Fornal and E. Pierre, *Asymmetric dark matter from gravitational waves*, Phys. Rev. D **106** (2022) 115040 [arXiv:2209.04788] [INSPIRE].

[65] O. Pujolas and G. Zahariade, *Domain wall annihilation: A QFT perspective*, Phys. Rev. D **107** (2023) 123527 [arXiv:2212.11204] [INSPIRE].

[66] G.B. Gelmini, J. Hyman, A. Simpson and E. Vitagliano, *Primordial black hole dark matter from catastrogenesis with unstable pseudo-Goldstone bosons*, JCAP **06** (2023) 055 [arXiv:2303.14107] [INSPIRE].

JHEP11(2023)169

[67] B. Fornal, K. Garcia and E. Pierre, *Testing unification and dark matter with gravitational waves*, *Phys. Rev. D* **108** (2023) 055022 [arXiv:2305.12566] [INSPIRE].

[68] J. Bosch, Z. Delgado, B. Fornal and A. Leon, *Gravitational wave signatures of gauged baryon and lepton number*, *Phys. Rev. D* **108** (2023) 095014 [arXiv:2306.00332] [INSPIRE].

[69] S. Blasi, R. Jinno, T. Konstandin, H. Rubira and I. Stomberg, *Gravitational waves from defect-driven phase transitions: domain walls*, *JCAP* **10** (2023) 051 [arXiv:2302.06952] [INSPIRE].

[70] S. Blasi and A. Mariotti, *Domain Walls Seeding the Electroweak Phase Transition*, *Phys. Rev. Lett.* **129** (2022) 261303 [arXiv:2203.16450] [INSPIRE].

[71] S. Blasi, A. Mariotti, A. Rase, A. Sevrin and K. Turbang, *Friction on ALP domain walls and gravitational waves*, *JCAP* **04** (2023) 008 [arXiv:2210.14246] [INSPIRE].

[72] S.F. King, D. Marfatia and M.H. Rahat, *Towards distinguishing Dirac from Majorana neutrino mass with gravitational waves*, arXiv:2306.05389 [INSPIRE].

[73] A. Vilenkin and E.P.S. Shellard, *Cosmic Strings and Other Topological Defects*, Cambridge University Press (2000).

[74] K. Saikawa, *A review of gravitational waves from cosmic domain walls*, *Universe* **3** (2017) 40 [arXiv:1703.02576] [INSPIRE].

[75] T. Hiramatsu, M. Kawasaki and K. Saikawa, *Gravitational Waves from Collapsing Domain Walls*, *JCAP* **05** (2010) 032 [arXiv:1002.1555] [INSPIRE].

[76] T. Hiramatsu, M. Kawasaki, K. Saikawa and T. Sekiguchi, *Axion cosmology with long-lived domain walls*, *JCAP* **01** (2013) 001 [arXiv:1207.3166] [INSPIRE].

[77] T. Hiramatsu, M. Kawasaki and K. Saikawa, *On the estimation of gravitational wave spectrum from cosmic domain walls*, *JCAP* **02** (2014) 031 [arXiv:1309.5001] [INSPIRE].

[78] R.D. Peccei and H.R. Quinn, *CP Conservation in the Presence of Instantons*, *Phys. Rev. Lett.* **38** (1977) 1440 [INSPIRE].

[79] R.D. Peccei and H.R. Quinn, *Constraints Imposed by CP Conservation in the Presence of Instantons*, *Phys. Rev. D* **16** (1977) 1791 [INSPIRE].

[80] S. Weinberg, *A New Light Boson?*, *Phys. Rev. Lett.* **40** (1978) 223 [INSPIRE].

[81] F. Wilczek, *Problem of Strong P and T Invariance in the Presence of Instantons*, *Phys. Rev. Lett.* **40** (1978) 279 [INSPIRE].

[82] P. Svrcek and E. Witten, *Axions In String Theory*, *JHEP* **06** (2006) 051 [hep-th/0605206] [INSPIRE].

[83] A. Arvanitaki, S. Dimopoulos, S. Dubovsky, N. Kaloper and J. March-Russell, *String Axiverse*, *Phys. Rev. D* **81** (2010) 123530 [arXiv:0905.4720] [INSPIRE].

[84] B. Holdom and M.E. Peskin, *Raising the Axion Mass*, *Nucl. Phys. B* **208** (1982) 397 [INSPIRE].

[85] B. Holdom, *Strong QCD at High-energies and a Heavy Axion*, *Phys. Lett. B* **154** (1985) 316 [*Erratum ibid.* **156** (1985) 452] [INSPIRE].

[86] J.M. Flynn and L. Randall, *A Computation of the Small Instanton Contribution to the Axion Potential*, *Nucl. Phys. B* **293** (1987) 731 [INSPIRE].

[87] V.A. Rubakov, *Grand unification and heavy axion*, *JETP Lett.* **65** (1997) 621 [hep-ph/9703409] [INSPIRE].

JHEP11(2023)169

[88] K. Choi and H.D. Kim, *Small instanton contribution to the axion potential in supersymmetric models*, *Phys. Rev. D* **59** (1999) 072001 [hep-ph/9809286] [INSPIRE].

[89] Z. Berezhiani, L. Gianfagna and M. Giannotti, *Strong CP problem and mirror world: The Weinberg-Wilczek axion revisited*, *Phys. Lett. B* **500** (2001) 286 [hep-ph/0009290] [INSPIRE].

[90] A. Hook, *Anomalous solutions to the strong CP problem*, *Phys. Rev. Lett.* **114** (2015) 141801 [arXiv:1411.3325] [INSPIRE].

[91] H. Fukuda, K. Harigaya, M. Ibe and T.T. Yanagida, *Model of visible QCD axion*, *Phys. Rev. D* **92** (2015) 015021 [arXiv:1504.06084] [INSPIRE].

[92] S. Dimopoulos, A. Hook, J. Huang and G. Marques-Tavares, *A collider observable QCD axion*, *JHEP* **11** (2016) 052 [arXiv:1606.03097] [INSPIRE].

[93] P. Agrawal and K. Howe, *Factoring the Strong CP Problem*, *JHEP* **12** (2018) 029 [arXiv:1710.04213] [INSPIRE].

[94] M.K. Gaillard, M.B. Gavela, R. Houtz, P. Quilez and R. Del Rey, *Color unified dynamical axion*, *Eur. Phys. J. C* **78** (2018) 972 [arXiv:1805.06465] [INSPIRE].

[95] J. Preskill, M.B. Wise and F. Wilczek, *Cosmology of the Invisible Axion*, *Phys. Lett. B* **120** (1983) 127 [INSPIRE].

[96] L.F. Abbott and P. Sikivie, *A Cosmological Bound on the Invisible Axion*, *Phys. Lett. B* **120** (1983) 133 [INSPIRE].

[97] M. Dine, W. Fischler and M. Srednicki, *A Simple Solution to the Strong CP Problem with a Harmless Axion*, *Phys. Lett. B* **104** (1981) 199 [INSPIRE].

[98] M. Dine and W. Fischler, *The Not So Harmless Axion*, *Phys. Lett. B* **120** (1983) 137 [INSPIRE].

[99] P. Arias, D. Cadamuro, M. Goodsell, J. Jaeckel, J. Redondo and A. Ringwald, *WISPy Cold Dark Matter*, *JCAP* **06** (2012) 013 [arXiv:1201.5902] [INSPIRE].

[100] P. Sikivie, *Of Axions, Domain Walls and the Early Universe*, *Phys. Rev. Lett.* **48** (1982) 1156 [INSPIRE].

[101] G.B. Gelmini, M. Gleiser and E.W. Kolb, *Cosmology of Biased Discrete Symmetry Breaking*, *Phys. Rev. D* **39** (1989) 1558 [INSPIRE].

[102] K.A. Beyer and S. Sarkar, *Ruling out light axions: The writing is on the wall*, *SciPost Phys.* **15** (2023) 003 [arXiv:2211.14635] [INSPIRE].

[103] J. Preskill, S.P. Trivedi, F. Wilczek and M.B. Wise, *Cosmology and broken discrete symmetry*, *Nucl. Phys. B* **363** (1991) 207 [INSPIRE].

[104] K. Nakayama, F. Takahashi and N. Yokozaki, *Gravitational waves from domain walls and their implications*, *Phys. Lett. B* **770** (2017) 500 [arXiv:1612.08327] [INSPIRE].

[105] M.C. Huang and P. Sikivie, *The Structure of Axionic Domain Walls*, *Phys. Rev. D* **32** (1985) 1560 [INSPIRE].

[106] S.A. Abel, S. Sarkar and P.L. White, *On the cosmological domain wall problem for the minimally extended supersymmetric standard model*, *Nucl. Phys. B* **454** (1995) 663 [hep-ph/9506359] [INSPIRE].

[107] A.J. Long, *Cosmological Aspects of the Clockwork Axion*, *JHEP* **07** (2018) 066 [arXiv:1803.07086] [INSPIRE].

JHEP11(2023)169

[108] Z. Chen, A. Kobakhidze, C.A.J. O'Hare, Z.S.C. Picker and G. Pierobon, *Cosmology of the companion-axion model: dark matter, gravitational waves, and primordial black holes*, arXiv:2110.11014 [INSPIRE].

[109] G. Grilli di Cortona, E. Hardy, J. Pardo Vega and G. Villadoro, *The QCD axion, precisely*, *JHEP* **01** (2016) 034 [arXiv:1511.02867] [INSPIRE].

[110] A. Vilenkin and A.E. Everett, *Cosmic Strings and Domain Walls in Models with Goldstone and PseudoGoldstone Bosons*, *Phys. Rev. Lett.* **48** (1982) 1867 [INSPIRE].

[111] S.M. Barr, K. Choi and J.E. Kim, *Some aspects of axion cosmology in unified and superstring models*, *Nucl. Phys. B* **283** (1987) 591 [INSPIRE].

[112] E.P.S. Shellard, *Axionic domain walls and cosmology*, in *27th Liege International Astrophysical Colloquium on Origin and Ea Early History of the Universe*, Liege, Belgium (1986) [INSPIRE].

[113] S.M. Barr, K. Choi and J.E. Kim, *Some aspects of axion cosmology in unified and superstring models*, *Nucl. Phys. B* **283** (1987) 591 [INSPIRE].

[114] S. Chang, C. Hagmann and P. Sikivie, *Studies of the motion and decay of axion walls bounded by strings*, *Phys. Rev. D* **59** (1999) 023505 [hep-ph/9807374] [INSPIRE].

[115] M. Gorghetto, E. Hardy and G. Villadoro, *Axions from Strings: the Attractive Solution*, *JHEP* **07** (2018) 151 [arXiv:1806.04677] [INSPIRE].

[116] M. Hindmarsh, J. Lizarraga, A. Lopez-Eiguren and J. Urrestilla, *Scaling Density of Axion Strings*, *Phys. Rev. Lett.* **124** (2020) 021301 [arXiv:1908.03522] [INSPIRE].

[117] M. Gorghetto, E. Hardy and G. Villadoro, *More axions from strings*, *SciPost Phys.* **10** (2021) 050 [arXiv:2007.04990] [INSPIRE].

[118] M. Gorghetto and E. Hardy, *Post-inflationary axions: a minimal target for axion haloscopes*, *JHEP* **05** (2023) 030 [arXiv:2212.13263] [INSPIRE].

[119] B.S. Ryden, W.H. Press and D.N. Spergel, *The evolution of networks of domain walls and cosmic strings*, Technical Report CFA-3011 [INSPIRE].

[120] M. Hindmarsh, *Analytic scaling solutions for cosmic domain walls*, *Phys. Rev. Lett.* **77** (1996) 4495 [hep-ph/9605332] [INSPIRE].

[121] T. Garagounis and M. Hindmarsh, *Scaling in numerical simulations of domain walls*, *Phys. Rev. D* **68** (2003) 103506 [hep-ph/0212359] [INSPIRE].

[122] J.C.R.E. Oliveira, C.J.A.P. Martins and P.P. Avelino, *The Cosmological evolution of domain wall networks*, *Phys. Rev. D* **71** (2005) 083509 [hep-ph/0410356] [INSPIRE].

[123] P.P. Avelino, J.C.R.E. Oliveira and C.J.A.P. Martins, *Understanding domain wall network evolution*, *Phys. Lett. B* **610** (2005) 1 [hep-th/0503226] [INSPIRE].

[124] A.M.M. Leite and C.J.A.P. Martins, *Scaling Properties of Domain Wall Networks*, *Phys. Rev. D* **84** (2011) 103523 [arXiv:1110.3486] [INSPIRE].

[125] A. Vilenkin, *Gravitational Field of Vacuum Domain Walls and Strings*, *Phys. Rev. D* **23** (1981) 852 [INSPIRE].

[126] F. Ferrer, E. Masso, G. Panico, O. Pujolas and F. Rompineve, *Primordial Black Holes from the QCD axion*, *Phys. Rev. Lett.* **122** (2019) 101301 [arXiv:1807.01707] [INSPIRE].

JHEP11(2023)169

[127] J.R. Espinosa, T. Konstandin, J.M. No and G. Servant, *Energy Budget of Cosmological First-order Phase Transitions*, JCAP **06** (2010) 028 [arXiv:1004.4187] [INSPIRE].

[128] S.M. Barr and D. Seckel, *Planck scale corrections to axion models*, Phys. Rev. D **46** (1992) 539 [INSPIRE].

[129] M. Kamionkowski and J. March-Russell, *Planck scale physics and the Peccei-Quinn mechanism*, Phys. Lett. B **282** (1992) 137 [hep-th/9202003] [INSPIRE].

[130] R. Holman, S.D.H. Hsu, T.W. Kephart, E.W. Kolb, R. Watkins and L.M. Widrow, *Solutions to the strong CP problem in a world with gravity*, Phys. Lett. B **282** (1992) 132 [hep-ph/9203206] [INSPIRE].

[131] Z.G. Berezhiani, R.N. Mohapatra and G. Senjanovic, *Planck scale physics and solutions to the strong CP problem without axion*, Phys. Rev. D **47** (1993) 5565 [hep-ph/9212318] [INSPIRE].

[132] S. Ghigna, M. Lusignoli and M. Roncadelli, *Instability of the invisible axion*, Phys. Lett. B **283** (1992) 278 [INSPIRE].

[133] G. Senjanovic, *Discrete symmetries, strong CP problem and gravity*, in *4th Hellenic School on Elementary Particle Physics*, Corfu, Greece (1992) [hep-ph/9311371] [INSPIRE].

[134] B.A. Dobrescu, *The Strong CP problem versus Planck scale physics*, Phys. Rev. D **55** (1997) 5826 [hep-ph/9609221] [INSPIRE].

[135] T. Banks and N. Seiberg, *Symmetries and Strings in Field Theory and Gravity*, Phys. Rev. D **83** (2011) 084019 [arXiv:1011.5120] [INSPIRE].

[136] M. Kawasaki, K. Saikawa and T. Sekiguchi, *Axion dark matter from topological defects*, Phys. Rev. D **91** (2015) 065014 [arXiv:1412.0789] [INSPIRE].

[137] L. Di Luzio, M. Giannotti, E. Nardi and L. Visinelli, *The landscape of QCD axion models*, Phys. Rept. **870** (2020) 1 [arXiv:2003.01100] [INSPIRE].

[138] D.J. Gross, R.D. Pisarski and L.G. Yaffe, *QCD and Instantons at Finite Temperature*, Rev. Mod. Phys. **53** (1981) 43 [INSPIRE].

[139] S. Borsanyi et al., *Calculation of the axion mass based on high-temperature lattice quantum chromodynamics*, Nature **539** (2016) 69 [arXiv:1606.07494] [INSPIRE].

[140] C.A.J. O'Hare, G. Pierobon, J. Redondo and Y.Y.Y. Wong, *Simulations of axionlike particles in the postinflationary scenario*, Phys. Rev. D **105** (2022) 055025 [arXiv:2112.05117] [INSPIRE].

[141] P.B. Arnold, *One loop fluctuation-dissipation formula for bubble wall velocity*, Phys. Rev. D **48** (1993) 1539 [hep-ph/9302258] [INSPIRE].

[142] A. Notari, F. Rompineve and G. Villadoro, *Improved Hot Dark Matter Bound on the QCD Axion*, Phys. Rev. Lett. **131** (2023) 011004 [arXiv:2211.03799] [INSPIRE].

[143] F. D'Eramo, F. Hajkarim and S. Yun, *Thermal QCD Axions across Thresholds*, JHEP **10** (2021) 224 [arXiv:2108.05371] [INSPIRE].

[144] N. Ganoulis and M. Hatzis, *Light scattering by an axionic domain wall*, Mod. Phys. Lett. A **1** (1986) 409 [INSPIRE].

[145] M.M. Forbes and A.R. Zhitnitsky, *Domain walls in QCD*, JHEP **10** (2001) 013 [hep-ph/0008315] [INSPIRE].